An ab Initio Study of the $[C_2H_5O^-]$ Potential Energy Surface and the Fragmentation Pathways of the Ethoxide Anion

S.-W. Chiu*

National Center for Supercomputing Applications and Department of Molecular and Integrative Physiology, University of Illinois, Urbana, Illinois 61801

Kai-Chung Lau and Wai-Kee Li*

Department of Chemistry, The Chinese University of Hong Kong, Shatin, N.T., Hong Kong

Received: February 26, 1999; In Final Form: May 14, 1999

The $[C_2H_5O^-]$ potential energy surface has been investigated with a modified Gaussian-2 methodology, the G2++ approximation. Eight stable $[C_2H_5O^-]$ isomers have been found on the surface: $CH_3CH_2O^-$ (**1**$^-$), W−CH_3CHOH^- (**2**$^-$), Y−CH_3CHOH^- (**3**$^-$), Y−$CH_2OCH_3^-$ (**4**$^-$), W−$CH_2OCH_3^-$ (**5**$^-$), ZE-$CH_2CH_2OH^-$ (**6**$^-$), EE-$CH_2CH_2OH^-$ (**7**$^-$), and EZ-$CH_2CH_2OH^-$ (**8**$^-$). Among these isomers, **1**$^-$ is the most stable thermodynamically. The calculated G2++ heats of formation for the isomeric anions are in very good accord with the available experimental data. Also studied with the same ab initio method are the various rearrangements among the eight isomers and the fragmentation pathways of **1**$^-$. Among the reactions involving **1**$^-$, the fragmentation process **1**$^- \rightarrow H_2 + CH_2CHO^-$ has the least barrier. This result is in total agreement with the experimental collision activated dissociation and infrared multiple photon induced elimination studies of the ethoxide anion.

Introduction

The gas-phase fragmentations of simple and more complex alkoxides have been well studied by both collision activated dissociation (CAD)[1−4] and infrared multiple photon (IRMP)[5−7] induced elimination techniques. Hayes et al.[1,2] investigated extensively the CAD of some simple alkoxides, e.g., ethoxide, propoxide, as well as butoxide, and suggested that the loss of neutral molecular hydrogen (H_2) from ethoxide and methane (CH_4) from butoxide proceed via a stepwise 1,2-elimination mechanism as illustrated below:

$$CH_3CH_2O^- \rightarrow [H^-\cdots(CH_3CHO)] \rightarrow [H_2\cdots(CH_2{=}CHO^-)] \rightarrow CH_2{=}CHO^- + H_2 \quad (1)$$

$$(CH_3)_3CO^- \rightarrow [CH_3\cdots(CH_3)_2CO^-] \text{ or } [CH_3^-\cdots(CH_3)_2CO] \rightarrow CH_3C(CH_2)O^- + CH_4 \quad (2)$$

Additionally, Raftery and co-workers[3] found that the loss of H_2 from complex alkoxide ions such as $Ph(CH_2)_nO^-$, where $n = 1-5$, may occur by similar 1,2-elimination mechanisms. From these CAD experiments, it was shown that different parent alkoxides gave rise to different fragmentation products. For instance, CAD studies of ethoxide, propoxide, and butoxide gave only the H_2 fragment in the spectra, and the CAD spectrum of *tert*-butoxide showed only CH_4 fragment, whereas the CAD spectra of iso-propoxide and iso-butoxide produced both H_2 and CH_4 fragments. Mercer et al.[4] also observed similar phenomenon in their CAD studies of C_2 to C_5 alkoxide ions and concluded that primary alkoxide ions fragmented by elimination of H_2 only, secondary alkoxide ions showed the elimination of both H_2 and alkane molecules (alkane molecules may usually be taken as CH_4 because the loss of CH_4 was more facile than the loss of larger alkanes), while tertiary alkoxide ions showed only the elimination of alkane. However, one may wonder why H_2 or CH_4 is preferentially eliminated from alkoxides, in view of that the fragmentations of H_2 or CH_4 from alkoxides are obviously competitive reactions. According to the CAD study of iso-propoxide ion, $(CH_3)_2CHO^-$, by Mercer et al.,[4] it was suggested that the preferential elimination of H_2 or CH_4 from iso-propoxide was due to the thermodynamic stabilities of the fragmentation intermediates involved, i.e., the energies of ion dipole complex $[H^-\cdots(CH_3)_2CO]$ for the elimination of H_2 and $[CH_3^-\cdots CH_3CHO]$ for the loss of CH_4. Besides, the feasibility of the isomeric rearrangements prior to fragmentation has not been taken into account in conjunction with the H_2 or CH_4 elimination reactions. Hence, to gain a better understanding of the fragmentation reactions, a comprehensive theoretical study on the various elimination mechanisms, as well as the isomeric rearrangements for alkoxide anions, is clearly desirable.

On the theoretical side, there have been a few ab initio studies on the fragmentation mechanisms of alkoxides. Hayes and co-workers[1,2] investigated the fragmentation mechanisms of H_2 from ethoxide and CH_4 from butoxide at the HF/4-31G and HF/6-311++G levels of theory. However, they did not consider the detail fragmentation intermediates involved nor the competitiveness of the fragmentation mechanisms between H_2 and CH_4 from the same alkoxide. In addition, there has not been any theoretical study on the isomeric rearrangements for alkoxides.

Therefore, on one hand, we propose to investigate both competitive fragmentation pathways of H_2 and CH_4 from ethoxide, $CH_3CH_2O^-$, with a modified Gaussian-2 (G2) procedure, to obtain and compare the G2 heats of reaction ($\Delta H°_r$) for these two fragmentation channels, as well as the G2 heats of formation ($\Delta H°_f$) for the fragmentation intermediates in-

10.1021/jp990702e CCC: $18.00
Published on Web 07/09/1999

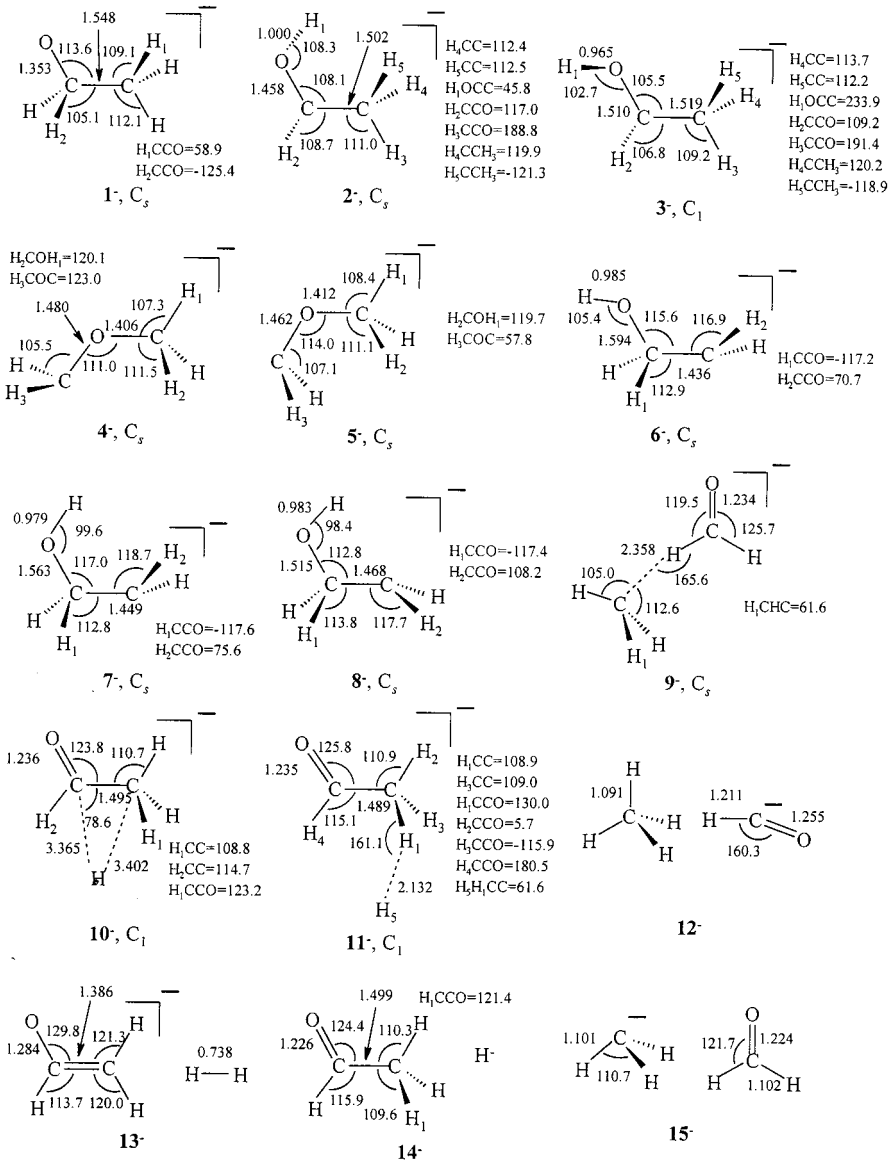

Figure 1. Selected structural parameters of $[C_2H_5O^-]$ isomers/conformers (**1**$^-$ to **8**$^-$), the fragmentation intermediates (**9**$^-$−**11**$^-$), and the fragments $CH_4 + HCO^-$ (**12**$^-$), $CH_2CHO^- + H_2$ (**13**$^-$), $CH_3CHO + H^-$ (**14**$^-$), and $CH_3^- + CH_2O$ (**15**$^-$), optimized at MP2(Full)/6-31++G(d) level. All bond lengths are in angstroms, and angles are in degrees.

volved. On the other hand, by the same modified G2 procedure, we also propose to study the isomeric rearrangements of $[C_2H_5O^-]$ anions by determining the geometries of the transition structures (TSs) as well as calculating the energy barriers. Finally, the potential energy surfaces (PESs) for the fragmentation pathways and isomerizations of $[C_2H_5O^-]$ anions will be described and discussed.

In the literature, there are two modified G2 methods, proposed by Gronert, for the studies of anionic species: the G2+[8] and the G2(dd)[9] methods. The G2+ approach involves single-point calculations at MP4/6-311+G(d,p), QCISD(T)/6-311+G(d,p), MP4/6-311+G(2df,p), and MP2/6-311+G(3df,2p) levels based on the geometries optimized at MP2/6-31+G(d,p) level of theory. On the other hand, the G2(dd) is an improved modification of G2+ approach, which additionally includes a second set of more diffuse sp-functions for first- and second-row elements.[9] However, both G2+ and G2(dd) approaches are specific for the study of the conjugate bases of the nonmetal hydrides, which are not within the scope of our study. As a result, we propose an alternative G2 method, called G2++, which is useful for studying ion−molecule reactions involving anions, particularly intermediates having H^- fragment. Methodological details of the G2++ model are discussed in the next section.

Theoretical Methods

All calculations were carried out on SGI10000 workstation and SGI Origin 2000 High Performance Server, using the Gaussian 94 package of programs.[10] In this work, a modified version of the G2 procedure,[11] denoted as the G2++ method, has been employed to approximate the energies of organic anions at the ab initio level of QCISD(T)/6-311++G(3df,2p). All structures have been optimized using the MP2 perturbation with all electrons included and employing the 6-31++G(d) basis set with diffuse functions included on both heavy and hydrogen atoms, i.e., at MP2(Full)/6-31++G(d). Besides, some alterations have been made on the single-point energy calculations in our proposed G2++ method, as compared with the conventional G2 procedure. Our method involves single-point energy calculations at QCISD(T)/6-311G(d,p), MP4/6-311G(d,p), MP4/6-311++G(d,p) [with additional diffuse functions for hydrogen atom], MP4/6-311G(2df,p), and MP2/6-311++G(3df,2p) [with

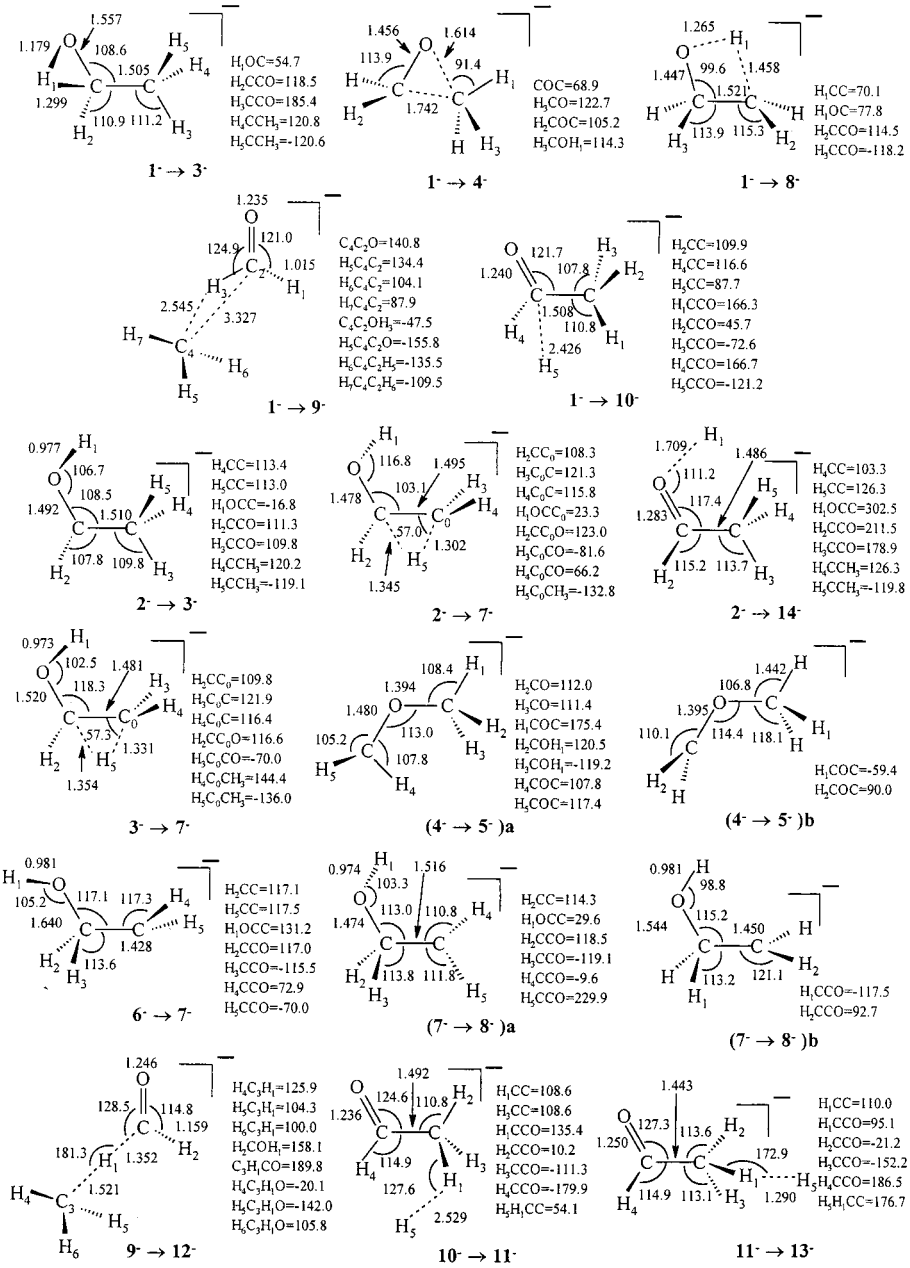

Figure 2. Selected structural parameters of various transition structures involving in the isomerizations and fragmentations of [$C_2H_5O^-$] anions, optimized at MP2(Full)/6-31++G(d) level. All bond lengths are in angstroms, and angles are in degrees.

additional diffuse functions for hydrogen atom]. A higher level correction (HLC) has been added to account for remaining basis set deficiencies. This is HLC $= -Bn_\beta - An_\alpha$, with $A = 0.18$, $B = 5.03$ mhartree (mh), n_α and n_β are the number of α and β valence electrons, respectively, and $n_\alpha \geq n_\beta$. The values of A and B are determined in the following manner. The value of A is arbitrarily set to be 0.18 mh, based on the difference between the exact and calculated energies of hydrogen atom. The value of B is then optimized to give zero mean deviation from experiment of the calculated atomization energies of 55 molecules having well-established experimental values.[11] The scaling factors of the MP2(Full)/6-31++G(d) vibrational frequencies for thermal correction and zero-point vibrational energies (ZPVE) correction have been determined in the following way. For thermal correction, the scaling factor (0.948) is obtained by minimizing the residuals[12] of the theoretical frequencies and the experimental fundamentals for the set of 24 molecules listed by Grev et al.[13] The experimental frequencies used are taken directly from a compendium compiled by Chase et al.[14] For ZPVE correction, the scaling factor (0.972) has been chosen to minimize the residuals of the theoretical and experimental ZPVEs. The experimental ZPVEs for the aforementioned set of 24 molecules are listed by Grev et al.[13] Finally, it is noted that all equilibrium and transition structures have been characterized by vibrational frequencies calculations at the MP2(Full)/6-31++G(d) level.

The G2++ heats of formation at temperature T ($\Delta H°_{fT}$) in this work are calculated in the following manner.[15] For molecule AB, its G2++ $\Delta H°_{fT}$ is calculated from the G2++ heat of reaction $\Delta H°_{rT}$(A + B→AB) and the respective experimental $\Delta H°_{fT}$(A) and $\Delta H°_{fT}$(B) for elements A and B. In the calculations of $\Delta H°_{rT}$ for anions, we set the $\Delta H°_{rT}$ value of a free election to be zero.

Results and Discussions

In our notations, single- or double-digit numerals with superscript "-" such as $\mathbf{1}^-$, $\mathbf{2}^-$, etc., refer to stable [$C_2H_5O^-$]

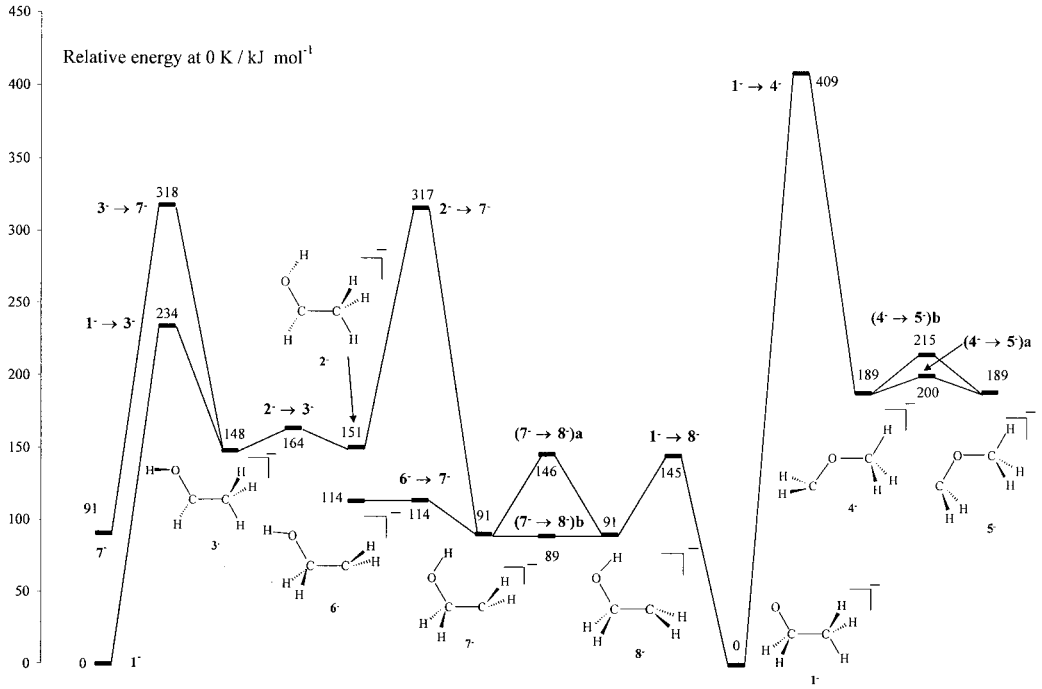

Figure 3. Schematic potential energy surface showing the intramolecular isomerization for $[C_2H_5O^-]$ anions. The geometries of all transition structures are shown in Figure 2.

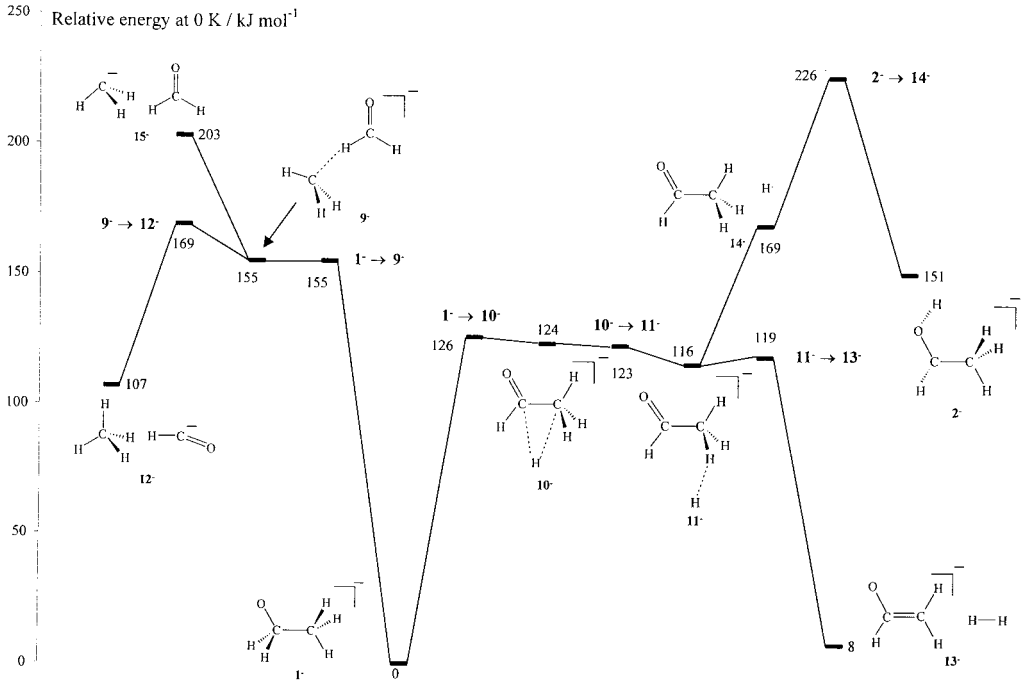

Figure 4. Schematic potential energy surface showing the fragmentation pathways for the ethoxide anion (**1**$^-$). The geometries of all transition structures are shown in Figure 2.

structures, fragmentation intermediates, or fragments. In addition, notations such as TS(**1**$^-$ → **2**$^-$) refer to the TS connecting **1**$^-$ and **2**$^-$.

The structures of the eight stable $[C_2H_5O^-]$ isomers/conformers (**1**$^-$ to **8**$^-$), and the three fragmentation intermediates (**9**$^-$ to **11**$^-$), as well as the four sets of fragments: $CH_4 + HCO^-$ (**12**$^-$), $CH_2CHO^- + H_2$ (**13**$^-$), $CH_3CHO + H^-$ (**14**$^-$), and $CH_3^- + CH_2O$ (**15**$^-$), are depicted in Figure 1. Figure 2 illustrates the geometries of the TSs for intramolecular isomerizations and molecular dissociations. The respective schematic PESs for the intramolecular isomerization and molecular fragmentations are displayed in Figures 3 and 4, respectively. The G2++ energies at 0 K (E_0), enthalpies at 298 K (H_{298}), heats of formation at 0 K ($\Delta H°_{f0}$) and 298 K ($\Delta H°_{f298}$) for $[C_2H_5O^-]$ isomers, fragmentation intermediates, and fragments are listed in Table 1. Tabulated in Table 2 are the G2++ energies and thermochemical data for various TSs. Additionally, it is noted that structural parameters and G2 energies for both $[C_2H_5O]$ radicals and $[C_2H_5O^+]$ cations can be found in a recent study[16] by Curtiss et al.

In the following discussion, when we quote the relative stabilities of isomers and conformers, as well as the barriers of reactions, we refer to the energy values at 0 K listed in Tables 1 and 2. On the other hand, when we quote the thermochemical

TABLE 1: G2++ Total Energies (E_0), Enthalpies (H_{298}), Standard Heats of Formation at 0 K ($\Delta H°_{f0}$), and 298 K ($\Delta H°_{f298}$) of [$C_2H_5O^-$] Isomers (1^-−8^-), Fragmentation Intermediates (9^-−11^-) and Fragments (12^-−15^-)

species	E_0 (hartree)	H_{298} (hartree)	$\Delta H°_{f0}$ (kJ mol^{-1})	$\Delta H°_{f298}$ (kJ mol^{-1})
$CH_3CH_2O^-$, (**1**$^-$)	−154.164 26	−154.159 45	−172.6	−186.1
				(−186 ± 10)[a]
				(−183 ± 9)[b]
W-CH_3CHOH^-, (**2**$^-$)	−154.106 89	−154.101 82	−22.0	−34.8
Y-CH_3CHOH^-, (**3**$^-$)	−154.107 71	−154.102 37	−24.1	−36.3
Y-$CH_2OCH_3^-$, (**4**$^-$)	−154.092 46	−154.086 87	15.9	4.4
				(−11 ± 9)[a]
W-$CH_2OCH_3^-$, (**5**$^-$)	−154.092 23	−154.086 94	16.5	4.2
				(−11 ± 9)[a]
ZE-$CH_2CH_2OH^-$, (**6**$^-$)	−154.120 99	−154.115 34	−59.0	−70.3
EE-$CH_2CH_2OH^-$, (**7**$^-$)	−154.129 67	−154.124 07	−81.8	−93.2
EZ-$CH_2CH_2OH^-$, (**8**$^-$)	−154.129 79	−154.124 38	−82.1	−94.1
[$CH_3^-\cdots H_2CO$], (**9**$^-$)	−154.105 11	−154.097 00	−17.3	−22.2
[$H\cdots CH_3CHO]^-$, (**10**$^-$)	−154.117 22	−154.110 49	−49.1	−57.6
[$H^-\cdots CH_3CHO$], (**11**$^-$)	−154.120 21	−154.113 62	−56.9	−65.8
$CH_4 + HCO^-$, (**12**$^-$)	−154.123 62	−154.116 00		
$CH_2CHO^- + H_2$, (**13**$^-$)	−154.161 31	−154.152 74		
$CH_3CHO + H^-$, (**14**$^-$)	−154.099 90	−154.092 63		
$CH_3^- + CH_2O$, (**15**$^-$)	−154.086 79	−154.079 09		

[a] Experimental result from ref 17. [b] Experimental result from ref 18.

TABLE 2: G2++ Total Energies (E_0), Enthalpies (H_{298}), Standard Heats of Formation at 0 K ($\Delta H°_{f0}$), and 298 K ($\Delta H°_{f298}$) of Various Transition Structures Involving in the Isomerizations and Fragmentations of [$C_2H_5O^-$] Anions

transition structures	E_0 (hartree)	H_{298} (hartree)	$\Delta H°_{f0}$ (kJ mol^{-1})	$\Delta H°_{f298}$ (kJ mol^{-1})
1$^-$ → **3**$^-$	−154.075 17	−154.070 15	61.3	48.3
1$^-$ → **4**$^-$	−154.008 61	−154.003 66	236.1	222.9
1$^-$ → **8**$^-$	−154.108 92	−154.104 09	−27.3	−40.8
1$^-$ → **9**$^-$	−154.105 42	−154.097 82	−18.1	−24.3
1$^-$ → **10**$^-$	−154.116 27	−154.110 80	−46.6	−58.4
2$^-$ → **3**$^-$	−154.101 83	−154.096 97	−8.7	−22.1
2$^-$ → **7**$^-$	−154.043 71	−154.038 54	143.9	131.3
2$^-$ → **14**$^-$	−154.078 04	−154.072 76	53.8	41.5
3$^-$ → **7**$^-$	−154.043 07	−154.037 68	145.6	133.6
(**4**$^-$ → **5**$^-$)**a**	−154.087 92	−154.083 15	27.8	41.2
(**4**$^-$ → **5**$^-$)**b**	−154.082 44	−154.077 06	42.2	30.2
6$^-$ → **7**$^-$	−154.120 76	−154.115 53	−58.4	−70.8
(**7**$^-$ → **8**$^-$)**a**	−154.108 57	−154.103 70	−26.4	−39.8
(**7**$^-$ → **8**$^-$)**b**	−154.130 22	−154.125 04	−83.2	−95.8
9$^-$ → **12**$^-$	−154.099 81	−154.092 70	−3.4	−10.9
10$^-$ → **11**$^-$	−154.117 50	−154.111 54	−49.8	−60.4
11$^-$ → **13**$^-$	−154.119 05	−154.113 65	−53.9	−65.9

data such as $\Delta H°_f$ of isomers and confomers, etc., we refer to the values at 298 K.

Stable Isomers and TSs for the [$C_2H_5O^-$] Anions. In this section, we discuss the stable isomers **1**$^-$ to **8**$^-$ and the various TSs linking them. The schematic PES for these isomers is shown in Figure 3.

The ethoxide anion, $CH_3CH_2O^-$ (**1**$^-$), the conjugate base of ethanol, is the most stable species among the eight [$C_2H_5O^-$] isomers. It has a staggered structure with C_s symmetry. With our G2++ method, the $\Delta H°_{f298}$ is calculated to be −186.1 kJ mol^{-1}, in excellent agreement with the two experimental values in the literature: −186 ± 10 [17] and −183 ± 9 [18] kJ mol^{-1}. On the other hand, we also obtained the G2 $\Delta H°_{f298}$ value (−183.8 kJ mol^{-1}) for **1**$^-$, which is also in very good accord with the experimental values.

The 1-hydroxyethyl anion, CH_3CHOH^-, has two conformers: W−CH_3CHOH^- (**2**$^-$) and Y−CH_3CHOH^- (**3**$^-$). Both conformers have C_1 symmetry and are less stable than **1**$^-$ by 151 and 149 kJ mol^{-1}, respectively, at the G2++ level. Interconversion of **2**$^-$ to **3**$^-$ can be achieved by rotation of the hydroxyl group around the CO bond. The TS for this rotation, TS(**2**$^-$→**3**$^-$), has been located, and the G2++ barrier is calculated to be 13 kJ mol^{-1} above **2**$^-$.

The methoxymethyl anion, $CH_2OCH_3^-$, also has two conformers: Y−$CH_2OCH_3^-$ (**4**$^-$) and W−$CH_2OCH_3^-$ (**5**$^-$). Both have C_s symmetry, and they also have similar thermal stabilities. Conformer **5**$^-$ is just slightly more stable than **4**$^-$ by 0.6 kJ mol^{-1} at 0 K. The respective G2++ $\Delta H°_{f298}$ for **4**$^-$ and **5**$^-$ are 4.4 and 4.2 kJ mol^{-1}. These two values are slightly out of the error range of the experimental $\Delta H°_{f298}$ (−11 ± 9 kJ mol^{-1} [17]) for $CH_2OCH_3^-$. However, it should be noted that the error range of conventional G2 procedure is at least ±10 kJ mol^{-1}. Interestingly, interconversion between **4**$^-$ and **5**$^-$ can be achieved via two TSs, TS(**4**$^-$ → **5**$^-$)**a**, and TS(**4**$^-$→**5**$^-$)**b**. The former (about 10 kJ mol^{-1} above **5**$^-$) involves the rotation of the methylene group around the CO bond, while the latter entails inversion at the methylenic carbon with a barrier of ca. 25 kJ mol^{-1} above **5**$^-$.

The 2-hydroxyethyl anion, $CH_2CH_2OH^-$, may exist in ZE (**6**$^-$), EE (**7**$^-$), and EZ (**8**$^-$) conformations. All these conformers have C_s symmetry. At the G2++ level, conformers **7**$^-$ and **8**$^-$ have similar stabilities with $\Delta H°_{f298}$ values of −93.2 and −94.1 kJ mol^{-1}, respectively. Meanwhile, conformer **6**$^-$ is about 23 kJ mol^{-1} less stable than **7**$^-$ and **8**$^-$. The interconversion TSs for **6**$^-$ → **7**$^-$ and **7**$^-$ → **8**$^-$ were located. Conversion **6**$^-$ → **7**$^-$ involves the rotation of the hydroxyl hydrogen around the CO bond; this rearrangement requires a negligible barrier of 0.5 kJ mol^{-1} above **6**$^-$. In conversion **7**$^-$ → **8**$^-$ via TS(**7**$^-$ → **8**$^-$)**a**, the methylene moiety rotates from trans arrangement to cis, and vice versa. The rotational barrier is calculated to be 55 kJ mol^{-1} at the G2++ level. An alternative route for this conversion proceeds through TS(**7**$^-$ → **8**$^-$)**b**, involving a simple inversion at the anionic center. The G2++ barrier is slightly negative for this particular case, indicating the barrier should be very small.

So far we have discussed the TSs involving interconversions of conformers and all these transformations have relatively small barriers, ranging from <1 to 55 kJ mol^{-1}. We now discuss the remaining TSs shown in Figure 3. All these TSs involve either methyl shift (**1**$^-$ → **4**$^-$) or hydrogen shift (**1**$^-$ → **3**$^-$, **1**$^-$ → **8**$^-$, **2**$^-$ → **7**$^-$, and **3**$^-$ → **7**$^-$) reactions. The barriers of these reactions are fairly large: 409 kJ mol^{-1} for reaction **1**$^-$ → **4**$^-$ and 234, 145, 166, and 170 kJ mol^{-1} for reactions **1**$^-$ → **3**$^-$, **1**$^-$ → **8**$^-$, **2**$^-$ → **7**$^-$, and **3**$^-$ → **7**$^-$, respectively. It is interesting to note

that there is no TS linking $\mathbf{1}^-$ and $\mathbf{7}^-$, or $\mathbf{1}^-$ and $\mathbf{6}^-$, due to the relative orientations of the hydrogens. To effect $\mathbf{1}^- \rightarrow \mathbf{6}^-$, we need to proceed via $\mathbf{1}^- \rightarrow \mathbf{8}^- \rightarrow \mathbf{7}^- \rightarrow \mathbf{6}^-$. To obtain $\mathbf{7}^-$ from $\mathbf{1}^-$, we can either proceed via $\mathbf{1}^- \rightarrow \mathbf{8}^- \rightarrow \mathbf{7}^-$ or $\mathbf{1}^- \rightarrow \mathbf{3}^- \rightarrow \mathbf{7}^-$, with the latter requiring a larger activation energy.

Fragmentation Pathways of the Ethoixde Anion ($\mathbf{1}^-$). Four fragmentation pathways of $\mathbf{1}^-$ were studied in this work: $\mathbf{1}^- \rightarrow \mathbf{12}^-$ ($CH_4 + HCO^-$), $\mathbf{1}^- \rightarrow \mathbf{13}^-$ ($CH_2CHO^- + H_2$), $\mathbf{1}^- \rightarrow \mathbf{14}^-$ ($CH_3CHO + H^-$), and $\mathbf{1}^- \rightarrow \mathbf{15}^-$ ($CH_3^- + CH_2O$). These pathways are summarized schematically in Figure 4.

Among these four fragmentations, both $\mathbf{1}^- \rightarrow \mathbf{12}^-$ and $\mathbf{1}^- \rightarrow \mathbf{15}^-$ involve complex [$CH_3^- \cdots CH_2O$] ($\mathbf{9}^-$), which is less stable than $\mathbf{1}^-$ by 155 kJ mol^{-1}. Complex $\mathbf{9}^-$ can be formed from $\mathbf{1}^-$ via TS($\mathbf{1}^- \rightarrow \mathbf{9}^-$) with a G2++ barrier of about 155 kJ mol^{-1}. Product $\mathbf{15}^-$ may be obtained from $\mathbf{9}^-$ by a simple bond cleavage reaction. The overall G2++ barrier of $\mathbf{1}^- \rightarrow \mathbf{15}^-$ is thus 203 kJ mol^{-1}. On the other hand, proton abstraction by CH_3^- within $\mathbf{9}^-$ through TS($\mathbf{9}^- \rightarrow \mathbf{12}^-$) requires relatively little energy (14 kJ mol^{-1}) and, in the process, CH_4 and HCO^- are produced. Thus the overall barrier for $\mathbf{1}^- \rightarrow \mathbf{12}^-$ is 169 kJ mol^{-1}.

Now we turn our attention to $\mathbf{1}^- \rightarrow \mathbf{13}^-$. As shown in Figure 4, the complex [$H^- \cdots CH_3CHO$] ($\mathbf{11}^-$) is formed from $\mathbf{1}^-$ via two TSs, TS($\mathbf{1}^- \rightarrow \mathbf{10}^-$) and TS($\mathbf{10}^- \rightarrow \mathbf{11}^-$), requiring an overall barrier of 126 kJ mol^{-1}. Proton abstraction by H^- within $\mathbf{11}^-$ produces H_2 and CH_2CHO^-, requiring very little energy (3 kJ mol^{-1}).

Finally, we discuss the fragmentation process of $\mathbf{1}^- \rightarrow \mathbf{14}^-$. Upon obtaining $\mathbf{11}^-$ from $\mathbf{1}^-$ in the aforementioned process, a simple dissociation of $\mathbf{11}^-$ produces CH_3CHO and H^-. The energy required is 53 kJ mol^{-1}. In other words, the overall energy barrier for $\mathbf{1}^- \rightarrow \mathbf{14}^-$ is 169 kJ mol^{-1}. Intuitively, $\mathbf{14}^-$ can also be formed from $\mathbf{1}^-$ by a simple bond cleavage reaction, which may or may not involve a TS. However, such a reaction is very likely to require more than 169 kJ mol^{-1} to proceed.

It is of interest to note H^- and CH_3CHO can recombine via TS($\mathbf{2}^- \rightarrow \mathbf{14}^-$) to form CH_3CHOH^- ($\mathbf{2}^-$), the energy barrier being 57 kJ mol^{-1}. Thus, the overall barrier for $\mathbf{1}^- \rightarrow \mathbf{2}^-$ is 226 kJ mol^{-1}, as shown in Figure 4. As can be seen in Figure 3, there is an alternative pathway for the transformation of $\mathbf{1}^- \rightarrow \mathbf{2}^-$; the barrier for this alternative route is 234 kJ mol^{-1}. In other words, the two routes have comparable barriers.

Comparing the barriers for the four fragmentation pathways studied as well as with those for the rearrangements involving $\mathbf{1}^-$, that of the hydrogen loss reaction, $\mathbf{1}^-$ ($CH_3CH_2O^-$) $\rightarrow \mathbf{13}^-$ ($H_2 + CH_2CHO^-$), requires the least energy (126 kJ mol^{-1}). This result is in total agreement with the CAD and IRMP studies of the ethoxide anion.[1,2] It is noted that the barriers of all rearrangements of $\mathbf{1}^-$ are larger than 126 kJ mol^{-1}. Only the rearrangement $\mathbf{1}^- \rightarrow \mathbf{8}^-$, with a barrier of 145 kJ mol^{-1}, is competitive with the fragmentation process $\mathbf{1}^- \rightarrow \mathbf{13}^-$.

In passing, combining the results of Figures 3 and 4, we note that $\mathbf{9}^-$ can be formed from $\mathbf{4}^-$ via a dissociation and recombination mechanism: $\mathbf{4}^-$ first dissociates to $\mathbf{15}^-$ (CH_2O and CH_3^-) and the two fragments then recombine to form $\mathbf{9}^-$.

Conclusion

The potential energy surface of [$C_2H_5O^-$] was studied by the ab initio G2++ method. Eight stable isomers were found on the surface: $CH_3CH_2O^-$ ($\mathbf{1}^-$), W−CH_3CHOH^- ($\mathbf{2}^-$), Y−CH_3CHOH^- ($\mathbf{3}^-$), Y−$CH_2OCH_3^-$ ($\mathbf{4}^-$), W−$CH_2OCH_3^-$ ($\mathbf{5}^-$), ZE-$CH_2CH_2OH^-$ ($\mathbf{6}^-$), EE-$CH_2CH_2OH^-$ ($\mathbf{7}^-$), and EZ-$CH_2CH_2OH^-$ ($\mathbf{8}^-$). The calculated heats of formation of these anions are in very good agreement with available experimental data. Among these isomers, $\mathbf{1}^-$ is the most stable species.

Additionally, the transition structures and barriers of the various rearrangements of the stable [$C_2H_5O^-$] anions were determined at the same level of theory. Also investigated were the following fragmentation processes of the ethoxide anion ($\mathbf{1}^-$): $\mathbf{1}^- \rightarrow CH_4 + HCO^-$, $\mathbf{1}^- \rightarrow CH_2CHO^- + H_2$, $\mathbf{1}^- \rightarrow CH_3CHO + H^-$, and $\mathbf{1}^- \rightarrow CH_3^- + CH_2O$. Among the fragmentation and rearrangement pathways involving $\mathbf{1}^-$, $\mathbf{1}^- \rightarrow CH_2CHO^- + H_2$ has the smallest barrier (126 kJ mol^{-1}). This result is in accord with the CAD and IRMP studies of the ethoxide anion.

Acknowledgment. S. W. C. acknowledges the use of computer time at the National Center for Supercomputing Application of the University of Illinois at Champaign-Urbana. K. C. L. and W. K. L. thank Computer Services Centre of The Chinese University of Hong Kong for generous allocation of computer time on the SGI Origin 2000 High Performance Server.

References and Notes

(1) Hayes, R. N.; Sheldon, J. C.; Bowie, J. H.; Lewis, D. E. *Aust. J. Chem.* **1985**, *38*, 1197.
(2) Hayes, R. N.; Sheldon, J. C.; Bowie, J. H.; Lewis, D. E. *J. Chem. Soc., Commun.* **1984**, 1431.
(3) Raftery, M. J.; Bowie, J. H.; Sheldon, J. C. *J. Chem. Soc., Perkin Trans. 2* **1988**, 563.
(4) Mercer, R. S.; Harrison, A. G. *Can. J. Chem.* **1988**, *66*, 2947.
(5) Tumas, W.; Foster, R. F.; Pellerite, M. J.; Brauman, J. I. *J. Am. Chem. Soc.* **1987**, *109*, 961.
(6) Tumas, W.; Foster, R. F.; Brauman, J. I. *J. Am. Chem. Soc.* **1984**, *106*, 4053.
(7) Tumas, W.; Foster, R. F.; Pellerite, M. J.; Brauman, J. I. *J. Am. Chem. Soc.* **1983**, *105*, 7464.
(8) Gronert S. *Chem. Phys. Lett.* **1996**, *252*, 415.
(9) Gronert S. *J. Am. Chem. Soc.* **1993**, *115*, 10258.
(10) Frisch, M. J.; Trucks, G. W.; Schlegel, H. B.; Gill, P. M. W.; Johnson, B. J.; Robb, M. A.; Cheeseman, J. R.; Keith, T. A.; Petersson, G. A.; Montgomery, J. A.; Raghavachari, K.; Al-Laham, M. A.; Zarkrewski, V. G.; Ortiz, J. V.; Foresman, J. B.; Cioslowski, J.; Stefanov, B. B.; Nanayakkara, A.; Challacombe, M.; Peng, C. Y.; Ayala, P. Y.; Chen, W.; Wong, M. W.; Andres, J. L.; Replogle, E. S.; Gomperts, R.; Martin, R. L.; Fox, D. J.; Binkley, J. S.; Defrees, D. J.; Baker, J.; Stewart, J. J. P.; Head-Gordon, M.; Gonzalez, C.; Pople, J. A. *GAUSSIAN* 94, Revision D4; Gaussian, Inc.: Pittsburgh, PA, 1995.
(11) Curtiss, L. A.; Raghavachari, K.; Trucks, G. W.; Pople, J. A. *J. Chem. Phys.* **1991**, *94*, 7221.
(12) Pople, J. A.; Scott, A. P.; Wong, M. W.; Radom, L. *Isr. J. Chem.* **1993**, *33*, 345.
(13) Grev, R. S.; Jansen, C. L.; Schaefer, H. F. *J. Chem. Phys.* **1991**, *95*, 5128.
(14) Chase, M. W.; Davies, C. A.; Downey, J. R.; Frurip, D. J.; McDonald, R. A.; Syverud, A. N. *J. Phys. Ref. Data* **1985**, *14* (Suppl. 1).
(15) Chiu, S.-W.; Cheung, Y.-S.; Ma, N. L.; Li, W.-K.; Ng, C. Y. *J. Mol. Struct. (THEOCHEM)* **1997**, *397*, 87.
(16) Curtiss, L. A.; Lucas, D. J.; Pople, J. A.; *J. Chem. Phys.* **1995**, *102*, 3292.
(17) Lias, S. G.; Bartmess, J. E.; Liebman, J. F.; Holmes, J. L.; Levin, R. D.; Mallard, W. G. *J. Phys. Chem. Ref. Data* **1988**, *17* (Suppl. 1).
(18) Haas, M. J.; Harrison, A. G. *Int. J. Mass Spectrom. Ion. Processes* **1993**, *124*, 115.